phys. stat. sol. (b) **245**, No. 5, 899–902 (2008) / **DOI** 10.1002/pssb.200778579

physica status solidi b
www.pss-b.com
basic solid state physics

White X-ray microdiffraction analysis of defects, strain and tilts in a free standing GaN film

R. I. Barabash[*, 1], G. E. Ice[1], B. A. Haskell[2], Shuji Nakamura[2], J. S. Speck[2], and W. Liu[3]

[1] Materials Science and Technology Division, Oak Ridge National Laboratory, Oak Ridge, TN 37831, USA
[2] Materials Department, College of Engineering, University of California at Santa Barbara, Santa Barbara, CA 93106, USA
[3] Advanced Photon Source, Argonne, IL, USA

Received 7 September 2007, accepted 3 March 2008
Published online 15 April 2008

PACS 61.05.cp, 68.55.–a, 81.05.Ea, 81.15.Kk

[*] Corresponding author: e-mail barabashr@ornl.gov, Phone: 865-2417230, Fax: 865-5747659

A novel white-beam microdiffraction analysis of defects, strains and tilts in a free standing *m*-plane GaN film grown via hydride vapor phase epitaxy is presented. It is shown that misfit dislocations are grouped within cell boundaries creating local lattice rotations (tilts) between the growing cells. Distribution of lattice rotations in the film is not homogeneous. Regions of large rotations are separated by low rotations regions. The dominating rotation axis is parallel [11$\bar{2}$0] direction. High in plane shear stress component is observed along [0001].

© 2008 WILEY-VCH Verlag GmbH & Co. KGaA, Weinheim

1 Introduction In the last several years rapid progress in GaN-based optoelectronic and electronic devices has been demonstrated. The main problems still limiting the optical properties of these diodes are caused by threading (TD) and misfit (MD) dislocations [1]. Recently developed cantilever epitaxial or pendeoepitaxial lateral overgrowth techniques significantly reduce the TD density [2–6]. However both methods are based on the growth of the wings of GaN overhanging over trenches in the substrate or GaN. The latter typically result in the formation of a wing tilt angle (WT) decreasing life expectancy of the optoelectronic devices [4–8]. Recently defect reduction in planar nonpolar (1$\bar{1}$00) *m*-plane GaN films was achieved via lateral epitaxial overgrowth by hydride vapor phase epitaxy [9–12].

2 Experiment The 120 µm thick GaN film was initially grown upon a (100) γ-$LiAlO_2$ substrate, which spontaneously separated from the film upon cooling from the 900 °C growth temperature. The average threading dislocation density in this sample, according to TEM analysis, was 4×10^9 cm^{-2} and the average stacking fault density was 1×10^5 cm. The Li concentration 2 µm from each surface according to SIMS depth profiling, was sharply different at 5×10^{17} atoms/cm^3 (back side) and 1×10^{15} (epi-surface) on the two faces. Comparable oxygen doping was observed on both surfaces. Further details on film growth can be found in Refs. [11] and [12].

The focused polychromatic synchrotron microbeam (PXM) method was used to determine 3D spatially resolved distribution of lattice rotations, dislocations, strain and stress fields in the sample. PXM uses a modified Laue diffraction technique based on polychromatic radiation [6–8, 13, 14]. Quantitative analysis of the Laue patterns yields the local lattice orientation (resolution ~0.01°) and deviatoric (shear) strain tensor (resolution ~10^{-4}). With PXM it is possible to quantitatively determine the GaN microstructure, local orientation and defects.

A laser confocal system (LEXT) was used to observe the microstructure of the surface of the film.

3 Results and discussion The in-plane microstructure of the free-standing film is shown in Fig. 1. As can be seen, the growth cells in plane are strongly elongated in one direction with a ratio of ~6 : 1. The out of plane dimension is ~120 µm and set by the thickness of the film. Neighbor growth cells are separated by cell boundaries (Fig. 1b).

WILEY InterScience® DISCOVER SOMETHING GREAT

© 2008 WILEY-VCH Verlag GmbH & Co. KGaA, Weinheim

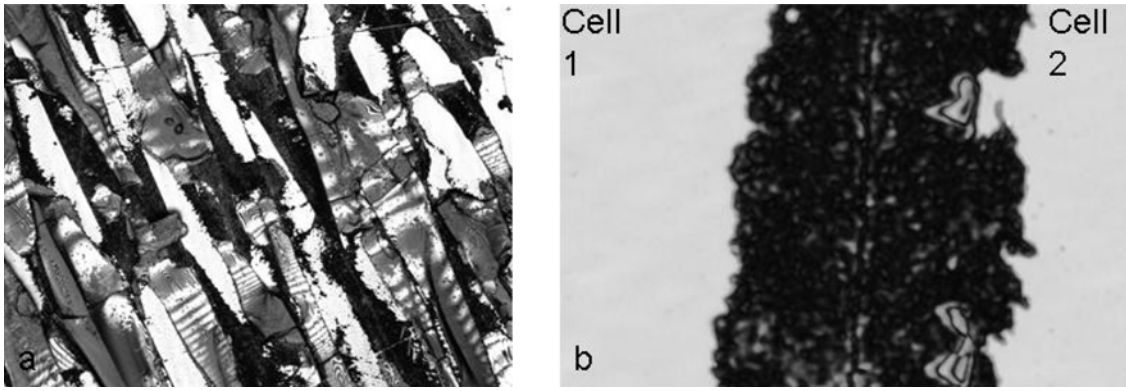

Figure 1 (a) Optical microstructure of the free standing film obtained with LEXT (magnification 1200); and a blown up boundary region between two growth cells (b).

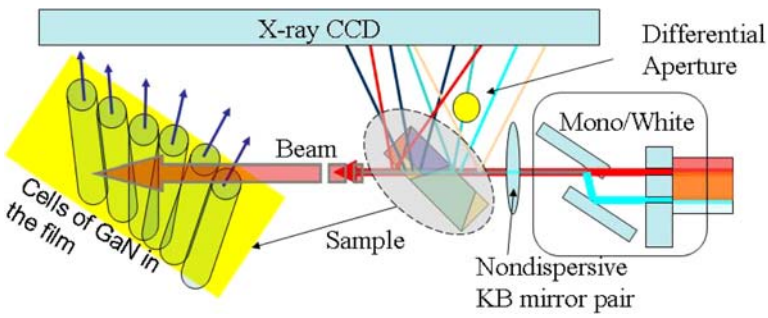

Figure 2 (online colour at: www.pss-b.com) Schematic of the relative orientation of the X-ray microbeam and a sample of the free standing GaN film with slightly misoriented growth cells. Due to high energy of the X-ray beam it penetrates through the thickness of the film.

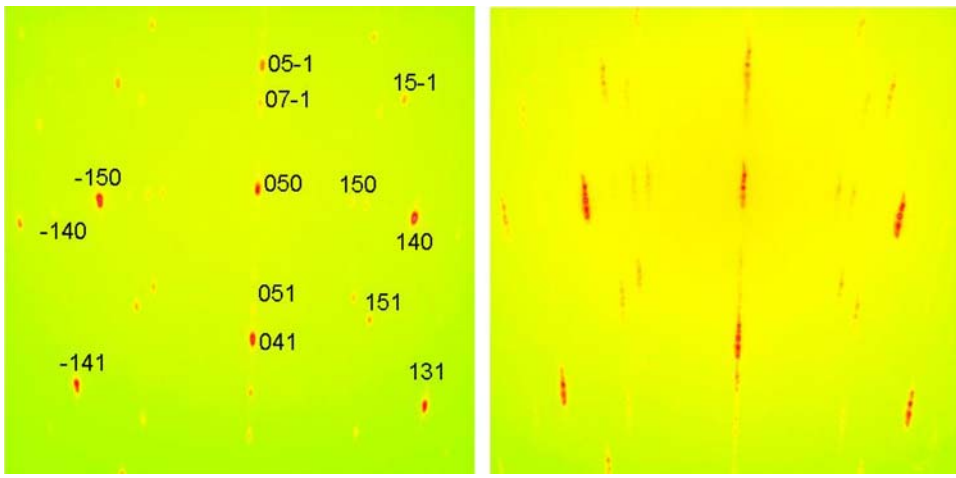

Figure 3 (online colour at: www.pss-b.com) Indexed Laue pattern from a region of the GaN film with a well defined orientation (left), and Laue pattern from a region with strongly misoriented growth cells (right). X-ray beam penetrates through several cells with different orientation and produces overlapping streaked Laue patterns from all cells it intercepts.

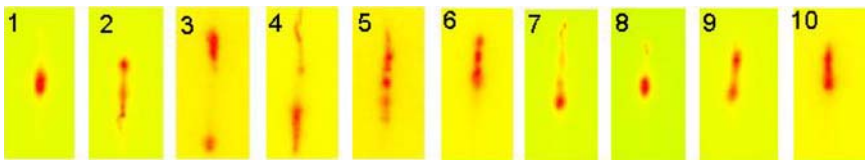

Figure 4 (online colour at: www.pss-b.com) Central $(05\bar{5}0)$ reflection at 10 different locations of the GaN film demonstrates orientation fluctuations of the surface normal.

© 2008 WILEY-VCH Verlag GmbH & Co. KGaA, Weinheim

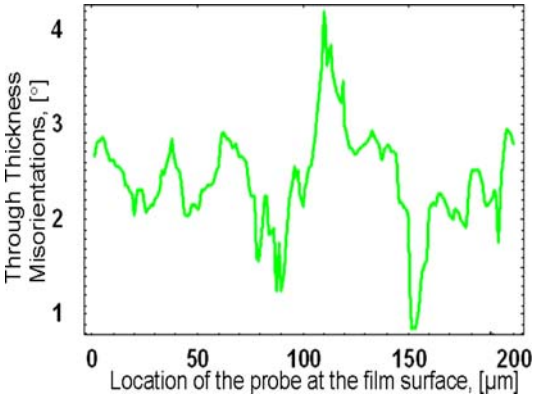

Figure 5 (online colour at: www.pss-b.com) Change of through thickness lattice misorientation as the probe is scanned horizontally parallel to film surface along the [0001] direction.

To understand the nature of the boundaries and probable defects formation, and determine crystallographic orientation of the growth cells, the film was further examined with PXM method. The focused polychromatic synchrotron microbeam (PXM) was diffracted from a submicrometer diameter area, producing complete diffraction patterns from the GaN film, which were collected by a charge-coupled device (CCD) area detector placed at an angle of 90° relative to the incident beam (Fig. 2).

Because the high-energy X-ray beam passes through the GaN film, the information is obtained from the whole thickness of the film (Fig. 3a and b). For this reason all reflections at the right frame of a Fig. 3 are elongated (streaked) and consist of several (up to 10) subpeaks. Each subpeak corresponds to a growth cell with distinct orientation. To demonstrate change of orientation within the probed region at different locations of the film, a 2D map was measured with PXM. During this measurement the polychromatic microbeam was scanned with a step size of 1 μm along each line at 260 locations perpendicular to the film buckling and totally 20 such parallel lines were measured. Figure 4 shows the central $(05\bar{5}0)$ Laue spot at 10 different locations. Well defined orientation through the film thickness results in a sharp spot (frame 1). Formation of sub-boundaries and/or disclination dipoles in (and between) the growth cells probed by the beam results in the abrupt change of orientation within the probed region and appearance of streaked reflections consisting of several sub-peaks. Distinct distances between subpeaks at different frames (Fig. 4) demonstrate variation in the tilt angle through the cell boundary.

Figure 5 plots the total integrated lattice misorientations through the film thickness as a function of position along a line perpendicular to the [0001] direction. At each position, the pencil beam penetrated through the film probing the variations in local crystal alignment. The beam penetrated though the whole film. A grid of 14 × 260 measurements was made with 1 μm pitch. As a result of such 2D mapping of the film surface the large-scale fluctuations of the local misorientations through the film thickness are revealed (Figs. 5 and 6). The wavelength of the fluctuations is ~25 μm. Figure 6 shows the inhomogeneous distribution of the local lattice rotations within a 260 × 14 μm region. Maximal misorientation (about 4.5°) corresponds to the red color of the map. It is apparent that distribution of misorientations is highly inhomogeneous. Extended regions of up to 80 μm in diameter with high misorientations are separated with more perfect regions with lower misorientations.

Lattice rotations are directly related to the distribution of geometrically necessary dislocations and boundaries [12, 13]. Abrupt rotations between the growth cells can be also described in terms of wedge disclination dipoles [4, 13]. The PXM results give a direct measurement of the misorientation between growth cells corresponding to the disclination dipole strength, ω. They show that the film rotates 1.5–4.5 degrees through of the film thickness. These rotations are accommodated by both local cell subboundaries and deviatoric strain within each cell. The latter in turn are accompanied by film buckling. The dominating rotation axis is parallel to $[11\bar{2}0]$ direction. There is little overall lattice rotation around the [0001] axis. In contrast the maximal shear is observed along [0001]. Lattice rotations indicate existence of a high level deviatoric (shear) stress field in the film. Relaxation of these stresses caused delamination of the film from the substrate and formation of multiple sub-boundaries, stacking faults and dislocations, causing local change of lattice orientation between and within the growing cells. Comparison with optical microstructure (Fig. 1) shows that the growth cells in the plane of the film are essentially anisotropic. They are about 5–7 times longer in $[11\bar{2}0]$ direction then in the orthogonal in-plane [0001] direction.

To obtain depth resolved information about the strain distribution in the GaN layers we performed measurements with the so called DAXM technique [13, 14] (Fig. 2). This special technique allows spatially resolved 3D measurements of strain as a function of depth in the film. The energy scan through the reflection $(05\bar{5}0)$ with maximal energy of 15.525 keV was performed with the so called "monowire" technique which indicated that the lattice pa-

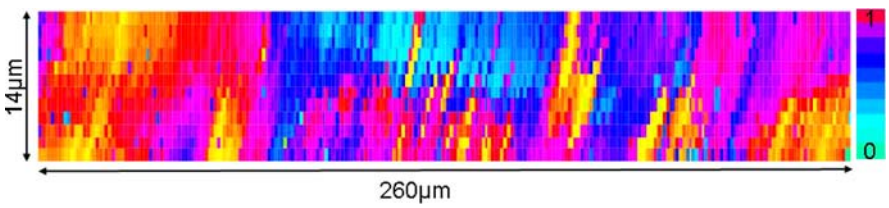

Figure 6 (online colour at: www.pss-b.com) Spatially resolved distribution of lattice misorientations in the free standing film.

© 2008 WILEY-VCH Verlag GmbH & Co. KGaA, Weinheim

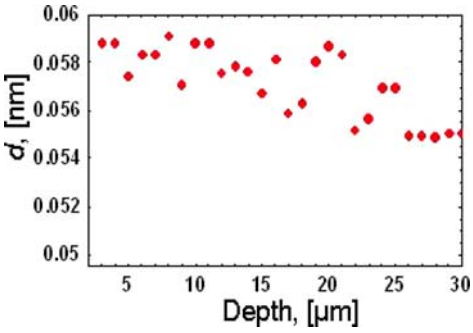

Figure 7 (online colour at: www.pss-b.com) Decrease of the $(05\bar{5}0)$ plane spacing through the depth of the film.

rameter changes more than 2% with the depth of the film (Fig. 7). Change in the lattice parameter through the film thickness indicates the existence of dilatational strain gradients in the Z-direction, ε_{ZZ}. Together with in-plane "misfit-induced" strain components ε_{XX} and ε_{YY}, ε_{ZZ} leads to the formation of a 3D stress field in the film. Relaxation of these stresses probably caused delamination of the film from the substrate and further buckling. From the direction of the rotation axes we can conclude that the maximum in-plane stress component occurred along [0001] direction due to larger ε_{XX} in-plain strain.

Simultaneously much higher in-plane ε_{XX} strain component partially suppressed cell growth in the [0001] direction and lead to the strong in-plane anisotropy of the growth cells.

Misorientation between growth cells was also observed in the wing region of the cantilever epitaxially grown films [6, 7].

4 Conclusion We argue that the sharp change of Li concentration through the film thickness, results in the strain gradient along the film normal. Together with in-plane "misfit strain" they form large 3D stress field distribution in the film. Growth cells are highly misoriented relative to each other. Misorientation angle fluctuates in the range of 1.5–4.5°. The rotation axis in the film is predominantly along $[11\bar{2}0]$ direction. The maximal in-plane shear stress component is observed in [0001] direction. Lattice rotations indicate existence of high level deviatoric (shear) stress field in the film. Relaxation of these stresses caused delamination of the film from the substrate and formation of multiple sub-boundaries, stacking faults, and dislocations causing local change of lattice orientation between and within the growing cells. Distinct in-plain strain components along $[11\bar{2}0]$ and [0001] directions result in the high in-plain anisotropy of the growth cells.

Acknowledgement Research sponsored in part by the Division of Materials Sciences and Engineering, Office of Basic Energy Sciences, U.S. Department of Energy, under Contract DE-AC05-00OR22725 with UT-Battelle, LLC. Data collection with PXM has been carried out on beamline ID-34-E at the Advanced Photon Source, Argonne IL. The APS is supported by the U.S. DOE, Basic Energy Sciences, Office of Science under contract No. W-31-109-ENG-38).

References

[1] T. Metzger, R. Hopler, and E. Born, Philos. Mag. A **77**, 1013 (1998).
[2] T. M. Katona, M. D. Craven, P. T. Fini, J. S. Speck, and S. P. DenBaars, Appl. Phys. Lett. **79**, 2907 (2001).
[3] T. M. Katona, J. S. Speck, and S. P. DenBaars, Appl. Phys. Lett. **81**, 3558 (2002).
[4] A. E. Romanov, P. Fini, and J. S. Speck, J. Appl. Phys. **93**, 106 (2003).
[5] P. Fini, A. Munkholm, C. Thomson, G. B. Stephenson, J. A. Eastman, M. V. Ramana Murty, O. Auciello, L. Zhao, S. P. DenBaars, and J. S. Speck, Appl. Phys. Lett. **76**, 3893 (2000).
[6] R. I. Barabash, G. E. Ice, W. Liu, C. Roder, S. Figge, S. Einfeldt, D. Hommel, T. M. Katona, J. S. Speck, S. P. DenBaars, and R. F. Davis, phys. stat. sol. (b) **243**(7), 1508–1513 (2006).
[7] R. I. Barabash, C. Roder, G. E. Ice, S. Einfeldt, J. D. Budai, O. M. Barabash, S. Figge, and D. Hommel, J. Appl. Phys. **100**, 053103 (2006).
[8] R. I. Barabash, G. E. Ice, C. Roder, J. D. Budai, W. Liu, S. Figge, S. Einfeldt, D. Hommel, and R. Davis, phys. stat. sol. (b) **244**, 1735 (2007).
[9] M. D. Craven, P. Waltereit, F. Wu, J. S. Speck, and S. P. DenBaars, Jpn. J. Appl. Phys. **42**, L235 (2003).
[10] A. Chakraborty, B. A. Haskell, S. Keller, J. S. Speck, S. P. DenBaars, S. Nakamura, and U. K. Mishra, Appl. Phys. Lett. **85**, 5143 (2004).
[11] B. A. Haskell, A. Chakraborty, F. Wu, H. Sasano, P. T. Fini, S. P. DenBaars, J. S. Speck, and Shuji Nakamura, J. Electron. Mater. **34**(4), 357–360 (2005).
[12] B. A. Haskell, T. J. Baker, M. B. McLaurin, F. Wu, P. T. Fini, S. P. DenBaars, J. S. Speck, and Shuji Nakamura, Appl. Phys. Lett. **86**, 111917 (2005).
[13] G. E. Ice and R. I. Barabash, White Beam Microdiffraction and Dislocations Gradient, in: Dislocations in Solids, Vol. 13, edited by F. R. N. Nabarro and J. P. Hirth (Elsevier, 2007), Chap. 79, pp. 499–602.
[14] B. C. Larson, W. Yang, G. E. Ice, J. D. Budai, and J. Z. Tischler, Nature **415**, 887 (2002).

© 2008 WILEY-VCH Verlag GmbH & Co. KGaA, Weinheim